Revista Mexicana de Astronomía y Astrofísica Revista mexicana de astronomía y astrofísica ISSN: 0185-1101

Universidad Nacional Autónoma de México, Instituto de Astronomía

Barani, C.; Martignoni, M.; Acerbi, F.; Michel, R.; Aceves, H.; Popov, V. Photometric Analysis of Two K Spectral Type Contact Binary Systems Revista mexicana de astronomía y astrofísica, vol. 58, no. 2, 2022, pp. 237-244 Universidad Nacional Autónoma de México, Instituto de Astronomía

DOI: https://doi.org/10.22201/ia.01851101p.2022.58.02.06

Available in: https://www.redalyc.org/articulo.oa?id=57175502006



Complete issue

More information about this article

Journal's webpage in redalyc.org



Scientific Information System Redalyc

Network of Scientific Journals from Latin America and the Caribbean, Spain and Portugal

Project academic non-profit, developed under the open access initiative

PHOTOMETRIC ANALYSIS OF TWO K SPECTRAL TYPE CONTACT BINARY SYSTEMS

C. Barani¹, M. Martignoni¹, F. Acerbi¹, R. Michel², H. Aceves², and V. Popov³

Received January 17 2022; accepted March 28 2022

ABSTRACT

The of the light of first analysis curves contact binaries ROTSE J135349.8+305205 (CB1) and 1SWASP J150957.5-115308 (CB2) using the Wilson-Devinney code is presented. Both binary systems are of the A-subtype with a shallow fill-out (20.8% and 15.8% respectively) and a difference in temperatures between the components of < 200 K. A mass-ratio of 0.302 is found for CB1, while for CB2 the interesting value of 0.904 is found. The short periods, 0.246 d for CB1 and 0.229 d for CB2, and their spectral type K suggests that these systems are near the shortest period limit. The absolute elements are estimated using GAIA parallaxes. CB2 is found to be at the beginning of its evolution, while CB1 will approach the final evolutionary stage. The sum of the component masses of CB1 is 0.813 M_{\odot} , below the mass limit of $1.0-1.2 M_{\odot}$ assumed for the known contact binary stars.

RESUMEN

Se presenta por primera vez el análisis, usando el código Wilson-Devinney, de las curvas de luz de las binarias de contacto ROTSE1 J135349.8+305205 (CB1) y 1SWASP J150957.5-115308 (CB2). Ambos sistemas son del subtipo-A con un relleno poco profundo (20.8% y 15.8%, respectivamente) y una diferencia en temperatura entre las componentes de $< 200\,\mathrm{K}$. Se encuentra que su razón de masas es de 0.302 para CB1, y para CB2 se encuentra el valor interesante de 0.904. Los periodos cortos, 0.246 d para CB1 y 0.229 d para CB2, y sus tipos espectrales K sugieren que estos sistemas están cercanos al límite de periodo más corto. Los elementos absolutos se estiman usando paralajes de GAIA. Se encuentra que CB2 está al comienzo del estadio evolutivo, mientras que CB1 se aproximará al estadío evolutivo final. La suma de las masas componentes de CB1 es 0.813 M_{\odot} , debajo del límite de $1.0-1.2\,\mathrm{M}_{\odot}$ que se supone para las binarias de contacto conocidas.

Key Words: techniques: photometric — binaries: contact — stars: individual: ROTSE J135349.8+305205, 1SWASP J150957.5-115308

1. INTRODUCTION

A contact binary (CB) is a close binary star system where both components interact strongly, fill out their Roche lobes and share a common envelope (Kopal 1959; Eggleton 2006). Thermal energy is transferred from the hotter (primary) to the colder (secondary) star mainly through the common envelope leading to the establishment of a similar tem-

perature of the two stars. However, their mass ratio can be rather different.

The observational study of contact binaries allows the testing of theoretical models helping us to further understand of –for example– the merging process of stars and the evolution of their common envelope.

Contact binary systems usually belong to spectral types F, G and K, with orbital periods less than a day. The K-type binaries have been expected to have periods shorter than 0.3 days and show shallow characteristics. The rarity of this kind of binaries makes them very interesting systems for testing the

¹Stazione Astronomica Betelguese, Magnago, Italy.

 $^{^2 {\}rm Instituto}$ de Astronomía, UNAM, Ensenada, Baja California, México.

³Department of Physics and Astronomy, Shumen University, Bulgaria.

thermal relaxation theory (TRO, Lucy 1976; Flannery 1976; Robertson & Eggleton 1977).

ROTSE J135349.8+305205 (hereafter J135349) was found to be variable during the ROTSE I all-sky survey (Akerlof et al. 2000) as an EW system with an orbital period of 0.24698301 d. After J135349 was discovered it remained a neglected object. Here, the light curves of J135349 are analyzed and presented for the first time.

A light curve for ROTSE J150957.5-115308 = V373 Lib (hereafter J150957) was reported by Lohr et al. (2013), which presented the typical EW-type behavior and an orbital period of 0.2290205 d. The official name was assigned in the 82nd name-list of variable stars (Kazarovets et al. 2019).

With no previous studies of both these systems, the aim of the present work is to analyze their light curves using the latest version of the Wilson-Devinney code (Wilson & Devinney 1971; Wilson 1994; Wilson & van Hamme. 2016) and to determine the Roche conguration and their orbital parameters.

The outline of the paper is as follows. In \S 2 we describe the observations made and their characteristics. In \S 3 the times of minima and new ephemeris for our two contact binaries are reported. In \S 4 the solution obtained with the Wilson-Devinney code is discussed and presented. In \S 5 an estimation of physical parameters using Gaia parallax data is presented. Finally, in \S 6 a discussion and final remarks are provided.

2. OBSERVATIONS

Observations done at the San Pedro Martir Observatory with the 0.84-m telescope, the Mexman filter-wheel and the *Spectral Instruments 1* CCD detector (an e2v CCD42-40 chip with a gain of 1.39 e⁻/ADU and readout noise of 3.54 e⁻). The field of view was $7.6' \times 7.6'$ and a binning of 2×2 was employed during all the observations.

J135349 was observed on April 26 2017 for 7.4h, May 4 2018 for 6.1h and April 4 2021 for 2.2h. Alternated exposures in filters B, V, R_c and I_c , with exposure times of 60, 40, 15 and 15 seconds respectively, were taken in all the observing runs.

J150957 was observed on February 21 2017 for 3.8h, February 23 2017 for 3.6h, March 4 2019 for 3.4h, June 6 2019 for 2.5h, April 11 2021 for 3.2h and April 13 2021 for 6.6h. Alternated exposures in filters B, V and R_c , with exposure times of 60, 35 and 20 seconds respectively, were taken in all the observing runs. Flat field and bias images were also taken during all the nights.

 $\begin{tabular}{ll} TABLE~1\\ TIMES~OF~MINIMA~FOR~J135349~AND~J150957\\ \end{tabular}$

HJD	Epoch(1)	O-C(1)	Error	Source
J135349:				
2457869.7252	-0.5	-0.0001	0.0013	TW^a
2457869.8489	0.0	0.0001	0.0015	"
2458242.8169	1510.0	-0.0008	0.0013	"
2458242.9419	1510.5	0.0008	0.0014	"
J150957:				
2455567.0550	0.0	-0.0026	0.0013	VSX^b
2457805.9514	9776.0	0.0030	0.0012	TW^a
2457808.0127	9785.0	0.0031	0.0012	"
2458640.8387	13421.5	0.0011	0.0012	"
2459315.9845	16369.5	-0.0013	0.0017	"
2459317.8165	16377.5	-0.0015	0.0021	"
2459317.9308	16378.0	-0.0017	0.0015	"

^aTW=This work. ^bVSX=Variable Star Index.

All images were processed using IRAF⁴ routines. Images were bias subtracted and flat field corrected before the instrumental magnitudes were computed with the standard aperture photometry method. These fields were also calibrated in the $UBV(RI)_c$ system with the help of some Landolt's photometric standards.

Based on the previous information, we decided to use star WISEJ135355.54+304735.9 (U=18.042, B=16.936, V=15.839, $R_c=15.148$ and $I_c=14.549$) as comparison star for J135349 since it has a similar color (making differential extinction corrections negligible). For the case of J150957, star WISEJ150953.24-115045.3 (U=15.398, B=14.587, V=13.589, $R_c=12.931$ and $I_c=12.446$) was employed. Any part of the data can be provided upon request.

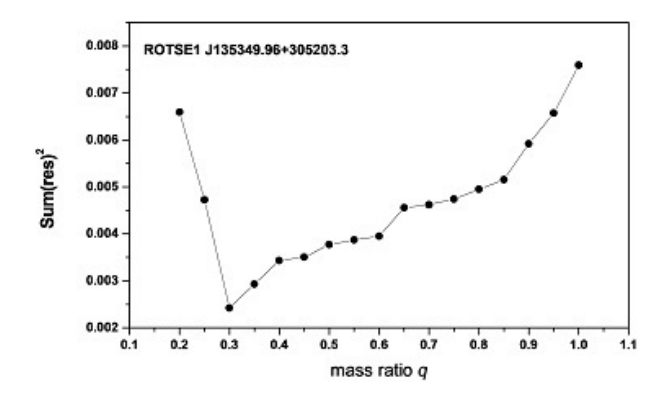
3. TIMES OF MINIMA AND NEW EPHEMERIS

From our observations we were able to obtain 4 times of minimum (ToM) for J135349 and 6 for J150957, one ToM has been found in literature. All ToMs are presented in Table 1.

All ToMs are heliocentric and determined by the polynomial fit method. With these data we updated the ephemeris as follows. For J135349

$$Min.I(HJD) = 2457869.8488(5) + 0^{d}.24699835(5) \times E,$$
 (1)

⁴IRAF is distributed by the National Optical Observatories, operated by the Association of Universities for Research in Astronomy, Inc., under cooperative agreement with the National Science Foundation.



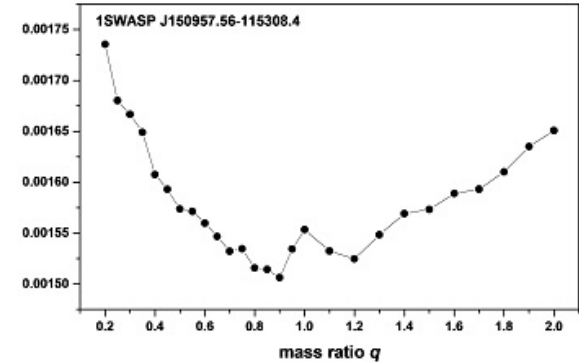


Fig. 1. The relation $\Sigma(res)^2$ versus mass ratio $q = M_2/M_1$ in Mode 3 of the W-D code for J135349 and J150957.

and for J150957

$$Min.I(HJD) = 2455567.0576(23) + 0^d.2290191(1) \times E.$$
 (2)

4. PHOTOMETRIC SOLUTION WITH THE W-D METHOD

The light curves of both systems show clearly the EW behavior with continuous changes in the light. For this reason the Mode 3 of the Wilson-Devinney (W-D) code was used in the calculation.

Using our observations, we were able to determine the color index of both systems and, from the tables of Worthey & Lee (2011), the temperature of the primary component; that was xed at 4760 K for J135349, and 4220 K for J150957.

The temperatures of the components of the two systems suggest convective envelopes. Hence, we adopted the following atmospheric parameters: the gravity-darkening coecients $g_1 = g_2 = 0.32$ (Lucy 1967) and the bolometric albedos $A_1 = A_2 = 0.5$ (Ruciński 1973) were assigned; the limb-darkening parameters originate from van Hamme (1993) for $\log g = 4.0$, and solar abundances.

During the dierential correction calculation in the W-D code we left as adjustable parameters the orbital inclination i, the mean surface eective temperature of the secondary component T_2 , the dimensionless surface potentials of the primary and secondary stars $\Omega_1 = \Omega_2$, the monochromatic luminosity of the primary component L_1 and the third light L_3 . In our solutions, we nd that the contribution of the third light is negligible.

The classical q-search method was used to nd the best initial value of the mass ratio to be used during the light curve analysis. The value of the mass ratio q was fixed in each iteration and increased after the

TABLE 2 LIGHT CURVES SOLUTION

	J135349	Error	J150957	Error
<i>i</i> (°)	77.384	0.340	65.226	0.062
T_1 (K)	4760	fixed	4220	fixed
T_2 (K)	4690	14	4032	9
$\Omega_1 = \Omega_2$	2.6064	0.0120	3.5144	0.0023
q	0.3023	0.0047	0.9048	0.0011
f	0.209	0.006	0.158	0.008
L_{1B}	0.6673	0.0049	0.5478	0.0039
L_{2B}	0.2535	0.0051	0.3254	0.0036
L_{1V}	0.6809	0.0046	0.5306	0.0033
L_{2V}	0.2636	0.0044	0.3478	0.0031
L_{1R}	0.6739	0.0043	0.5388	0.0027
L_{2R}	0.2650	0.0040	0.3660	0.0026
L_{1I}	0.6849	0.0041	-	-
L_{2I}	0.2728	0.0037	-	-
Primary				
r (pole)	0.4481	0.0026	0.3748	0.0003
$r ext{ (side)}$	0.4735	0.0035	0.3961	0.0004
r (back)	0.5023	0.0049	0.4320	0.0006
Secondary				
r (pole)	0.2861	0.0041	0.3582	0.0003
$r ext{ (side)}$	0.2991	0.0051	0.3777	0.0004
r (back)	0.3365	0.0093	0.4147	0.0006
$\Sigma (Res)^2$	0.0023052		0.0014944	

sum of residuals showed a minimum number. As one can see from Figure 1, where the sum of squares of residuals $(\Sigma(res)^2)$ versus mass ratio q is shown, the best mass ratio for J135349 is found at q=0.3 and for J150957 at q=0.9. These values of q were also treated as free parameters in the successive step of our analysis.

The final results obtained are listed in Table 2, while the obtained fit is shown in Figure 2.

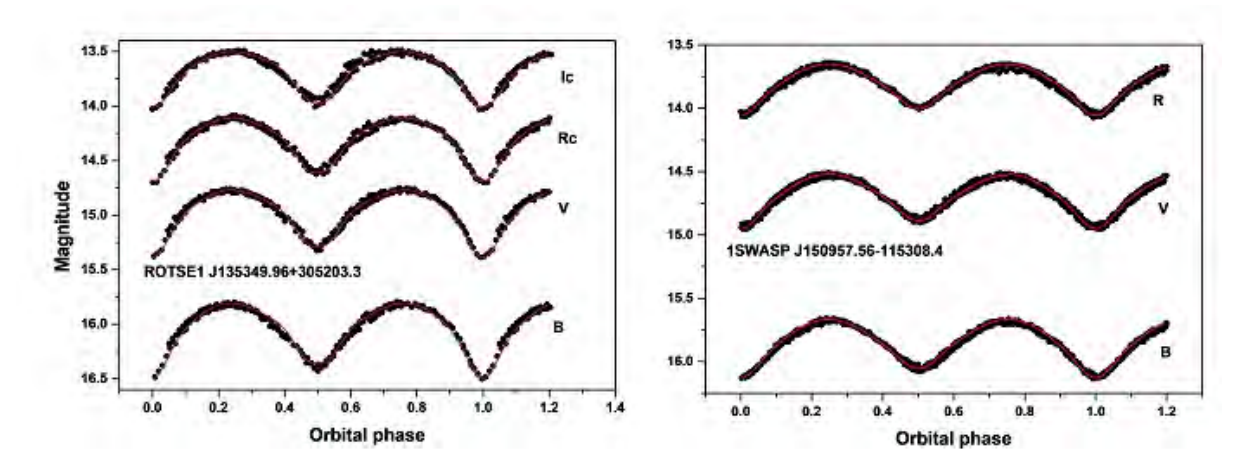


Fig. 2. CCD filtered light curves for the systems at different wavelengths. Points are the original observations while lines represent the theoretical light curves obtained in our modeling. The color figure can be viewed online.

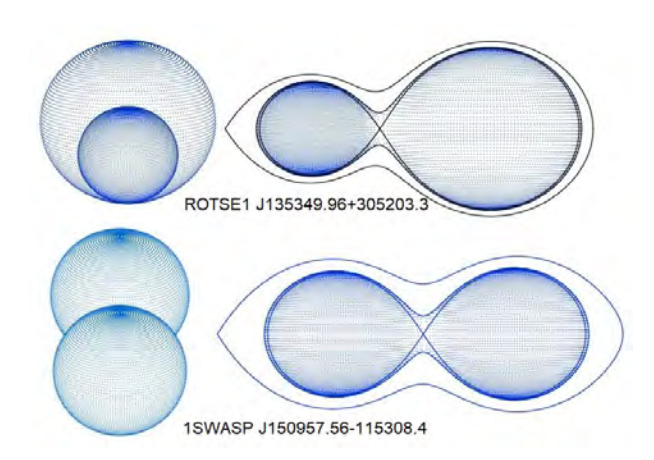


Fig. 3. Model representation of the CBs J135349 (q=0.3) and J150957 (q=0.9). The configuration at the primary minimum (left) and the Roche geometry (right) of these systems resulting from our modeling are shown. The color figure can be viewed online.

The values of the mass ratio for both systems indicate that they are typical A-subtype contact binaries in the Binnendijk (1965) classification. In Figure 3 the graphical representation of the systems and the relative Roche geometries are displayed.

By examining Table 2 the following information can be obtained. Both systems are of the A-subtype and in good thermal contact. The temperature of the components suggests that they are of the K spectral type. We note that it is somewhat strange to find a spectral K-type in A-subtype contact systems.

Systems of late spectral type generally belong to the W-subtype of W UMa contact binaries, but there are some exceptions that belong to the A-subtype as 2MASS J11201034-2201340 (Hu et al. 2016), ES Cep (Zhu et al. 2014), NSV 395 (Samec et al. 2016), and AP UMi (Awadalla et al. 2016).

Our two systems, despite having temperatures consistent with late spectral type K, show the characteristics of the subtype-A contact binaries; i.e., $T_1 > T_2$, transit at primary minimum, and a mass ratio q < 1.

CB J150957, having a mass ratio near unity, can be considered to be a high mass ratio system. High mass ratio systems, proposed firstly by Csizmadia & Klagyivik (2004) are a subgroup of contact binaries with mass ratio q > 0.72.

For the H-type the rate of energy transfer is less efficient than for other contact binaries at a given luminosity ratio. Having a mass ratio close to unity, less luminosity should be transferred in order to equalize their surface temperature.

Both binary systems show a low fill-out value. The low fill-out value is not a common feature among A-subtype contact binaries, and only a few A-subtype contact binaries are found to have a high mass ratio and a shallow common envelope (see Table 5 of Han et al. 2019). Contact binary J150957, which shows the same peculiar characteristics, can be added to this short list.

Note that the errors of the parameters given in Table 2 are the formal errors from the W-D code. For a discussion see Barani et al. (2017).

5. ESTIMATION OF THE PHYSICAL PARAMETERS WITH THE GAIA PARALLAX

Physical parameters such as mass, radius and luminosity are very important information for a contact binary system. Hence it is necessary to es-

timate them. Here we will indicate how we have estimated the physical parameters of J135349 and J150957 without radial velocity curves, using the parallax known by Gaia (Gaia Collaboration et al. 2018).

First, we calculated the Galactic extinction obtained using different methods from which an average value of the $A_{\rm V}$ (Masda et al. 2018) was extracted; in detail:

- 1. Simple and spiral model from Amôres & Lépine (2005) using the code GALExtin.⁵
- 2. Equation 1 from Iglesias-Marzoa et al. (2019).
- Dust tables by Schlegel et al. (1998) in the NASA IPAC (NASA 2015); proceeding therefore to deredden the visual magnitudes in quadratures.⁶

Using the parallax from Gaia we calculated the visual absolute magnitude using the relation

$$M_{\rm V} = m_{\rm V}({\rm max}) - 5\log D + 5 - A_{\rm V},$$
 (3)

and the bolometric magnitude $M_{\rm bol} = M_{\rm V} + BC_{\rm V}$, where $BC_{\rm V}$ is the bolometric correction obtained from the Pecaut et al. (2012) and Pecaut & Mamajek (2013) tables. This allowed us to obtain the total luminosity of the systems as

$$L_{\rm T} = L_1 + L_2 = 10^{-0.4(M_{\rm bol} - 4.7554)}$$
, (4)

and also the individual luminosities of the components.

Knowing the temperatures of the first and second component of each system we obtained their radii, and finally the total mass of the system; by using the value of the mass ratio obtained from the Wilson-Devinney analysis, the single masses M_1 and M_2 as shown in Table 3 were obtained.

We used the absolute elements of the primary and secondary components of both systems (Table 3) to estimate their evolutionary status by means of the $\log T_{\rm eff} - \log L$ (i.e. HertzsprungRussell) diagram on the evolutionary tracks of Girardi et al. (2000). The results are shown in Figure 4.

It is possible to see from Figure 4 that both the primary and the secondary components of J150957 are undermassive, with a luminosity comparable to that of a zero age main sequence (ZAMS) star.

For J135349 the primary component is located in the region between the ZAMS and TAMS (terminal

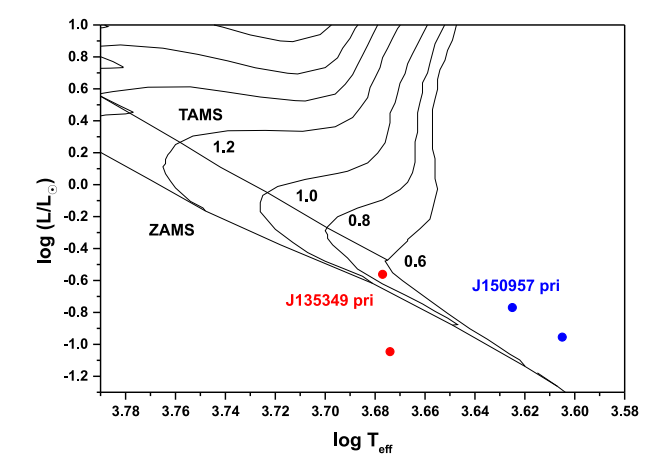


Fig. 4. Components of our binary systems plotted in the HR diagram. Zero age main sequence (ZAMS), terminal age main sequence (TAMS), evolutionary tracks and isochrones were taken from Girardi et al. (2000) for a solar chemical composition. The numbers denote initial masses. The color figure can be viewed online.

age main sequence) near the evolutionary track of 0.6, but it is underluminous given its mass. The secondary component, located under the ZAMS, is overmassive and slightly underluminous.

These results suggest that both systems consist of two stars of similar surface brightness, but in dierent evolutionary stages.

According to Flannery (1976) the stability parameter \Im for the mass-exchange in a CB can dened as:

$$\Im = \ln \left[\frac{R_p(0.38 + 0.2\log q)}{R_s(0.38 - 0.2\log q)} \right] , \tag{5}$$

where $R_{\rm p}$ refers to the primary's radius and $R_{\rm s}$ to the secondary. If $\Im=0$ no mass transfer occurs; if $\Im>0$ an unbalanced pressure gradient will force gas from the primary to secondary, and vice versa if $\Im<0$.

In our case we obtain $\Im=0.074$ for J150957; hence there is mass transfer from primary to the secondary; the contrary is true for J135349 were we obtain $\Im=-0.019$. In both CBs the value of \Im indicates a poor mass exchange between the components.

6. DISCUSSION AND FINAL REMARKS

The results of our analysis lead to two contact binary systems of the A-subtype that are in good thermal contact and have a shallow degree of contact between their components.

J150957, with a mass ratio q = 0.905, belongs to the high mass ratio type contact binaries (i.e. an H-type).

⁵http://www.galextin.org/interstellar_extinction.php

 $^{^6} http://irsa.ipac.caltech.edu/applications/DUST$

Target	$L_1({ m L}_{\odot})$	$L_2({ m L}_{\odot})$	$R_1({ m R}_{\odot})$	$R_2({ m R}_{\odot})$
J150957	0.170 ± 0.003	0.111 ± 0.007	0.771 ± 0.007	0.684 ± 0.025
J135349	0.275 ± 0.005	0.090 ± 0.008	0.770 ± 0.007	0.448 ± 0.023
	$a({ m R}_{\odot})$	$M_1({ m M}_\odot)$	$M_2({ m M}_\odot)$	$\rho_1 \; ({\rm g \; cm^{-3}})$
J150957	1.922 ± 0.020	0.953 ± 0.030	0.862 ± 0.028	1.27
J135349	1.546 ± 0.020	0.624 ± 0.027	0.189 ± 0.011	1.92
	$\rho_2 \; (\mathrm{g \; cm^{-3}})$	Mag Max V	M_V	${ m M}_{bol}$
J150957	3.03	14.52	7.04	6.13
J130349	2.90	14.77	6.32	5.85
	J	$\log J$	$\log J_{lim}$	J_{lim}
J150957	5.11^{51}	51.71	51.78	6.06^{51}
J130349	9.71^{50}	50.99	51.17	1.48^{51}

TABLE 3
ESTIMATED ABSOLUTE ELEMENTS

The spectral type K for all the components of the binary systems is somewhat strange for the Asubtype, but there are few A-subtype systems of Ktype.

In our analysis we found no signicant evidence of spots on the surfaces of the two components, the OConnell effect. This fact could be explained by a period of magnetic quiescence in the CBs (Zhang et al. 2011).

Using the absolute elements provided in Table 3 the dynamical evolution of contact binaries can be inferred via the determination of the orbital angular momentum J_0 (Eker et al. 2006).

In Figure 5 it is possible to see the position our systems occupy in the $\log J_0 - \log M$ diagram. The curved borderline separates the detached from the contact region and provides a check of the Roche configurations of J150957 and J130349. The values of $\log J_0$ place J150597 near the borderline of this diagram, while J130349 is in the well defined region of contact systems.

An exhaustive characterization of contact binaries, via the period-temperature relation, was recently conducted by Qian et al. (2020). In Figure 6 (Figure 4 in the original paper) we show the position of J150957 and J135349 in the period-temperature plot. Systems near the lower line are marginal contact systems while systems near the upper line are deep-contact ones. Between the two lines there are normal contact systems.

J150957 is near the lower boundary at the beginning of the evolutionary stage of contact binary evolution (Figure 6). It is also shown in the

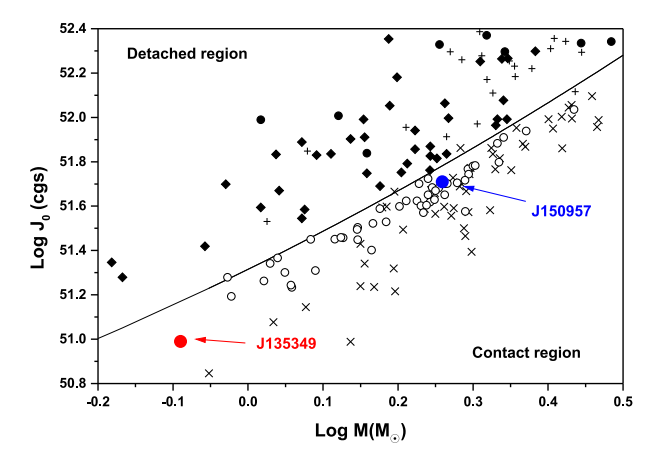


Fig. 5. Position of J150957 and J135349 in the $\log J_0 - \log M$ diagram. Symbols are described in Figure 1 of the original paper of Eker et al. (2006). The color figure can be viewed online.

 $\log J_0 - \log M$ plot where the system is slightly under the borderline, in the contact region. This assumption is endorsed by the high mass ratio (q = 0.9) and the low fill-out (15.6%).

The other system, J135349 is well inside the boundaries for normal EW (Figures 5 and 6) and, with its small mass ratio (q=0.38), its fill-out value (20.9%) and the almost equal temperature of the components, it follows that it is approaching the final evolutionary stage of the contact binary evolution.

The total mass determined for J150957 is over the minimum total mass limit for W UMa systems of 1.0-1.2 M_{\odot} (Stępień 2006), while J135349, with its total

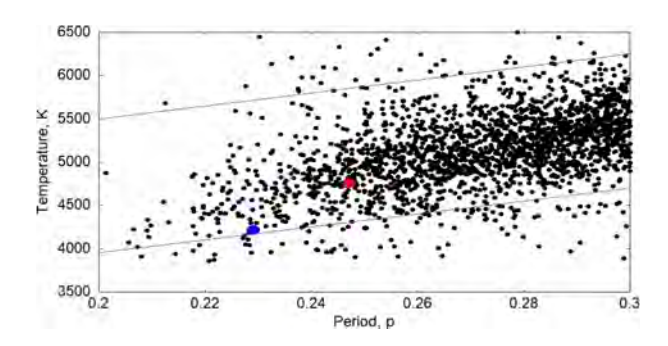


Fig. 6. Correlation between the orbital period P (days) and temperature T (K), based on parameters of 8510 contact binaries from Qian et al. (2020). The position J150957 is marked in blue, and that of J135349 in red. The color figure can be viewed online.

mass $M_{tot} = 0.813 \text{ M}_{\odot}$, is under this limit. This means a mass loss, and may imply a late evolutionary stage of this contact binary system.

This work made use of data from the European Space Agency (ESA) mission Gaia, ⁷ and processed by the Gaia Data Processing and Analysis Consortium (DPAC).⁸

Use of the International Variable Star Index (VSX) database has been made (operated at AAVSO Cambridge, Massachusetts, USA), as well as of the AAVSO Photometric All-Sky Survey (APASS) funded by the Robert Martin Ayers Sciences Fund. Also, use has been made of the VizieR catalogue access tool, CDS, Strasbourg, France. The original description of the VizieR service was published in A&AS 143, 23.

Based upon observations carried out at the Observatorio Astronómico Nacional on the Sierra San Pedro Mártir (OAN-SPM), Baja California, México.

REFERENCES

Akerlof, C., Amrose, S., Balsano, R., et al. 2000, AJ, 119, 1901, https://doi.org/10.1086/301321

Amôres, E. B. & Lépine, J. R. 2005, AJ, 130, 659, https://doi.org/10.1086/430957

Awadalla, N. S., Hanna, M. A., Ismail, M. N., Hassan, I. A., & Elkhamisy, M. A. 2016, JKAS, 49, 65, https://doi.org/10.5303/JKAS.2016.49.3.065

Barani, C., Martignoni, M., & Acerbi, F. 2017, NewA, 50, 73, https://doi.org/10.1016/j.newast.2016. 07.010

Binnendijk, L. 1965, The Position of Variable Stars in the Hertzsprung-Russell Diagram, VeBam, 27, 36 Csizmadia, S. & Klagyivik, P. 2004, A&A, 426, 1001, https://doi.org/10.1051/0004-6361:20040430

Eker, Z., Demircan, O., Bilir, S., & Karataş, Y. 2006, MNRAS, 373, 1483, https://doi.org/10.1111/j. 1365-2966.2006.11073.x

Eggleton, P. 2006, Evolutionary Processes in Binary and Multiple Stars, (Cambridge, UK: CUP)

Flannery, B. P. 1976, ApJ, 205, 217, https://doi.org/ 10.1086/154266

Gaia Collaboration, Brown, A. G. A., Vallenari, A., et al. 2018, A&A, 616, 1, https://doi.org/10.1051/0004-6361/201833051

Girardi, L., Bressan, A., Bertelli, G., & Chiosi, C. 2000, A&AS, 141, 371, https://doi.org/10.1051/ aas:2000126

Han, Q.-W., Li, L.-F., & Jiang, D.-K. 2019, RAA, 19, 174, https://doi.org/10.1088/1674-4527/19/ 12/174

Hu, C.-P., Yang, T.-C., Chou, Y., et al. 2016, AJ, 151, 170, https://doi.org/10.3847/0004-6256/151/6/

Iglesias-Marzoa, R., Arévalo, M. J., López-Morales, M., et al. 2019, A&A, 627, 153, https://doi.org/10.1051/0004-6361/201935516

Kazarovets, E. V., Samus, N. N., Durlevich, O. V., et al. 2019, IBVS, 6261, 1, https://doi.org/10.22444/ IBVS.6261

Kopal, Z. 1959, Close binary systems, (London, UK: The International Astrophysics Series, Chapman & Hall)

Lohr, M. E., Norton, A. J., Kolb, U. C., et al. 2013, A&A, 549, 86, https://doi.org/10.1051/ 0004-6361/201220562

Lucy, L. B. 1967, ZA, 65, 89

_____. 1976, ApJ, 205, 208, https://doi.org/10. 1086/154265

Masda, S. G., Al-Wardat, M. A., & Pathan, J. M. 2018, JApA, 39, 58, https://doi.org/10.1007/s12036-018-9548-z

Pecaut, M. J., Mamajek, E. E., & Bubar, E. J. 2012, ApJ, 746, 154, https://doi.org/10.1088/0004-637X/746/2/154

Pecaut, M. J. & Mamajek, E. E. 2013, ApJS, 208, 9, https://doi.org/10.1088/0067-0049/208/1/9

Qian, S.-B., Zhu, L.-Y., Liu, L., et al. 2020, RAA, 20, 163, https://doi.org/10.1088/1674-4527/20/10/163

Robertson, J. A. & Eggleton, P. P. 1977, MNRAS, 179, 359, https://doi.org/10.1093/mnras/179.3.359

Ruciński, S. M. 1973, AcA, 23, 79

Samec, R. G., Clark, J., Maloney, D., et al. 2016, JAAVSO, 44, 101

Schlegel, D. J., Finkbeiner, D. P., & Davis, M. 1998, ApJ, 500, 525, https://doi.org/10.1086/305772

Stepień, K. 2006, AcA, 56, 347

van Hamme, W. 1993, AJ, 106, 2096, https://doi.org/ 10.1086/116788

Wilson, R. E. & Devinney, E. J. 1971, ApJ, 166, 605, https://doi.org/10.1086/150986

⁷https://www.cosmos.esa.int/gaia.

 $^{^8 {\}rm https://www.cosmos.esa.int/web/gaia/dpac/consortium.}$

- Wilson, R. E. 1994, PASP, 106, 921, https://doi.org/ 10.1086/133464
- Wilson, R. E. & van Hamme, W. 2016, Computing Binary Stars Observables. <ftp.astro.ufl.edu>, directory pub/wilson/lcdc2015
- Worthey, G. & Lee, H.-ch. 2011, ApJS, 193, 1, https://doi.org/10.1088/0067-0049/193/1/1
- Zhang, X.-B., Ren, A.-B., Luo, C.-Q., & Luo, Y.-P. 2011, RAA, 11, 583, https://doi.org/10.1088/1674-4527/11/5/008
- Zhu, L. Y., Qian, S. B., Soonthornthum, B., et al. 2014, AJ, 147, 42, https://doi.org/10.1088/0004-6256/ 147/2/42

- F. Acerbi: Via Zoncada 51, Codogno, LO, 26845, Italy (acerbifr@tin.it).
- H. Aceves: Instituto de Astronomia, UNAM. A.P. 877, 22800 Ensenada, BC, Mexico (aceves@astro.unam.mx).
- C. Barani: Via Molinetto 35, Triulza di Codogno, LO, 26845, Italy (cvbarani@alice.it).
- M. Martignoni: Via Don G. Minzoni 26/D, Magnago, MI, 20020, Italy (massimiliano.martignoni@outlook.it).
- R. Michel: Instituto de Astronomia, UNAM. A.P. 877, 22800 Ensenada, BC, Mexico (rmm@astro.unam.mx).
- V. Popov: Department of Physics and Astronomy, Shumen University, 115 Universitetska str., 9700 Shumen, Bulgaria (velimir.popov@elateobservatory.com)